

Stochastic modeling of cohesive crack evolution in concrete using meshless interpolation techniques

Thomas Most, PhD Candidate

Institute of Structural Mechanics, Bauhaus-University Weimar, Germany

Christian Bucher, Supervisor

ABSTRACT: In this paper a discrete crack propagation algorithm is presented which uses a meshless discretization of the domain based on the Natural Neighbor Interpolation. The cohesive crack behavior of concrete is modeled with the Fictitious Crack Model representing a force transmission over micro cracks. A stress-based and an energy-based crack propagation criterion are presented and analyzed with several numerical examples, whereby the latter one led to more stable results. The material uncertainties in concrete are modeled with random fields by obtaining the characteristic structural response with Latin Hypercube Sampling. Finally the applicability of the stochastic model for the presented crack simulation is shown on an example.

1 INTRODUCTION

The discrete modeling of crack propagation in concrete with arbitrary geometries is still a field for many researchers because of the required discretization update of the domain. If standard finite elements are used, an adaptive remeshing of the structure is necessary. For higher order elements complex mesh generators are required. A younger technique is the Extended Finite Element Method [1], where the cracked elements are enriched by additional jump functions without remeshing, but the arbitrary intersection of cracks is limited through the predefined additional shape functions. In both techniques an adaptation of the integration point arrangement is necessary, which requires the transformation of the state variables. Due to the discontinuous stress distribution over element edges this procedure is not straightforward. An alternative possibility to model discrete cracks are meshless interpolation methods [2], where a predefined mesh is not necessary, the interpolation function depends only on the node positions. Most meshless interpolation functions can present continuous stress distributions almost everywhere, which makes the transformation of stress depending history variables much easier.

In this study the Natural Neighbor Interpolation [3] is used in a framework of a Galerkin approach. This methods shows several advantages compared to the common Element-free Galerkin Method [4]. To model the cohesive crack behavior of concrete the Fictitious Crack Model is applied [5], which assumes a force transmission over micro cracks. Two different crack propagation criteria will be presented and compared, a stress based criterion using a nonlocal average [6] of the stress tensor around the investigated point and an energy criterion based on the Virtual Crack Extension technique [7].

Due to the inhomogeneity of concrete, the material properties show much higher fluctuations compared to other materials which makes a stochastic modeling of the parameters reasonable. In this study isotropic random fields with several correlated parameters are used to describe the distribution of the different material quantities. In order to reduce the simulation effort the number of independent random variables is reduced through a spectral representation [8]. The statistical

analysis of the structural response is obtained by Latin Hypercube Sampling [9] which requires only a small number of samples compared to plain Monte Carlo Simulation [10]. The applicability of the presented algorithms will be shown on numerical examples.

2 MESHLESS INTERPOLATION

The common “Moving Least Squares” (MLS) interpolation, which is applied in the “Element-free Galerkin Method” [4], uses a base polynomial which is of lower order than the interpolated function. The system of equations becomes overdetermined and is solved by a least square approach by including a distance depending weighting function. The obtained interpolation function does not pass through the nodal values

$$\Phi_i^{MLS}(\mathbf{x}_j) \neq \delta_{ij} \quad (1)$$

therefore the MLS method is an approximation instead of a true interpolation. The essential boundary conditions are not fulfilled automatically, which needs special effort especially by using a coupling with finite elements.

A younger development in meshless methods is the application of the “Natural Neighbor Interpolation” [3] in the framework of a Galerkin approach, the so-called “Natural Neighbor Galerkin Method” or “Natural Element Method” (NEM) [11]. The interpolation technique defines natural neighbor nodes based on a Voronoi diagram of the domain. The dual of the Voronoi diagram is the Delaunay tessellation which is displayed in Figure 1 for a set of nodes. The interpolation of the displacements is done similarly to the Finite Element Method (FEM) by summing the nodal displacements \mathbf{u}_i multiplied with their shape function values Φ_i

$$\mathbf{u}^h(\mathbf{x}) = \sum_{i=1}^n \Phi_i(\mathbf{x}) \mathbf{u}_i \quad (2)$$

The NEM shape functions Φ_i are calculated from the area proportions of the second order Voronoi cells of the interpolation point as follows

$$\Phi_i(\mathbf{x}_{IP}) = \frac{A(\mathbf{x}_{IP,i})}{A(\mathbf{x}_{IP})}. \quad (3)$$

Figure 2 shows these second order Voronoi cells for a given interpolation point P_{IP} . A detailed description of the area computation by different algorithms is given in [12]. The Delaunay tessellation is assembled by using the “Triangle” software package [13].

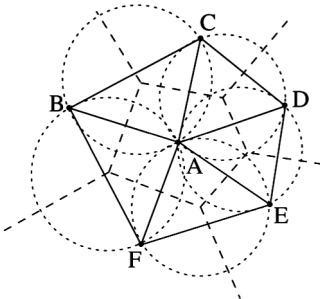


Figure 1. Voronoi diagram and corresponding Delaunay tessellation.

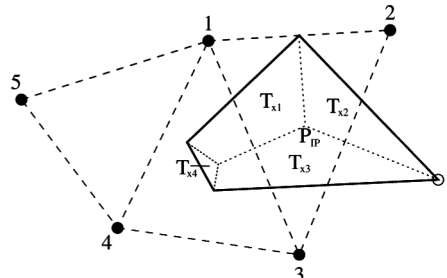


Figure 2. Second order Voronoi cells for sample interpolation point P_{IP} .

Contrary to the MLS-interpolation the NEM-interpolation represents the nodal values exactly

$$\Phi_i^{NEM}(\mathbf{x}_j) = \delta_{ij} \quad (4)$$

the essential boundary conditions are fulfilled automatically. The properties of the interpolation are linear completeness, linear precision at the boundaries [11] and C^1 continuity, except at the nodes, where we find C^0 continuity. To assemble the system matrices and vectors a numerical integration via Gauss point quadrature over the Delaunay triangles is used.

3 CRACK PROPAGATION MODELING

3.1 Cohesive crack model

To model the energy dissipation process in quasi-brittle materials such as concrete the Cohesive or Fictitious Crack Model [5] can be applied. It assumes the existence of a fracture process zone ahead of a real crack tip. Along the fictitious crack surfaces stresses can be transferred through mechanisms such as aggregate interlock and material bonding until the crack width reaches a critical value. The normal stress t_n is formulated as a function of the crack width w .

The stress state at such a cohesive crack tip is shown in Figure 3. In this study finite interface elements are used to transmit the cohesive forces between the meshless nodes at the crack surfaces, which are placed automatically during the crack growth simulation. The nodal discretization with the corresponding Delaunay triangles around a moving crack tip will be updated according to [14] where the author applied a local Laplace smoothing algorithm [15] to optimize the triangle integration zones for the MLS-interpolation. This concept is adapted to the NEM by investigating the smoothed triangles with respect to the fulfillment of the Delaunay criterion and their possible reassembling. The relation between the normal stress and the crack width is modeled with the common exponential softening law. In order to avoid the penetration of existing crack surfaces caused by reversed loading a penalty function is defined. The obtained relation for the normal stress is

$$t_n = \begin{cases} \left\{ f_{ct} \cdot \exp\left(-\frac{w \cdot c}{G_f - 0.5 \cdot f_{ct}^2 \cdot c^{-1}}\right) \right. & w \leq w_0 \\ & w_0 < w \leq w_c, \quad w_0 = \frac{f_{ct}}{c}, \quad w_c = 5 \frac{G_f}{f_{ct}} \\ & 0 & w > w_c \end{cases} \quad (5)$$

where G_f , f_{ct} and c are the specific fracture energy, the tensile strength and the penalty stiffness, respectively. The full normal stress is activated over a crack width w_0 . The critical crack opening w_c defines the point, where a micro cracks turns into a macro crack. For un- and reloading a linear function back to the point of origin is assumed. The complete normal stress function is displayed in Figure 4. The cohesive shear stress at the crack surfaces is modeled with the Coulomb friction hypothesis according to [16].

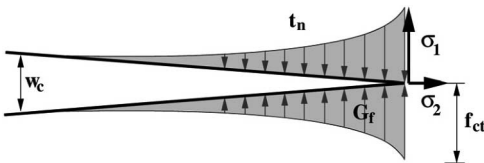


Figure 3. Stress state at the cohesive crack tip.

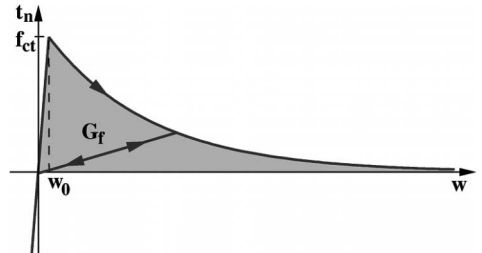


Figure 4. Normal stress function depending on crack opening displacement.

3.2 Stress-based crack propagation criterion

In many studies dealing with cohesive crack growth of concrete the Rankine criterion is applied (e.g. in [16] and in the contributions of C. Feist to [17]). By using this criterion a crack arises or grows if the maximum principal stress at the investigated point exceeds the tensile strength. The crack propagation direction is assumed to be perpendicular to this principal stress direction. In order to reduce the effects of load or geometry introduced singularities the computation of the stress tensor of the investigated point by a nonlocal average scheme is reasonable. This nonlocal stress tensor can be obtained as

$$\bar{\boldsymbol{\sigma}}(\mathbf{x}) = \int_{\Omega_E} \alpha(\mathbf{x}, \boldsymbol{\xi}) \cdot \boldsymbol{\sigma}(\boldsymbol{\xi}) d\boldsymbol{\xi}, \quad \alpha(\mathbf{x}, \boldsymbol{\xi}) = \frac{\alpha_\infty(\|\mathbf{x} - \boldsymbol{\xi}\|)}{\int_{\Omega_E} \alpha_\infty(\|\mathbf{x} - \boldsymbol{\zeta}\|) d\boldsymbol{\zeta}} \quad (6)$$

where α and Ω_E are the nonlocal weighting function and the nonlocal interaction area, respectively. As weighting function usually a bell shaped polynom is chosen [6], which depends on the distance $r = \|\mathbf{x} - \boldsymbol{\xi}\|$ and on an interaction radius R . Detailed information on the determination of this quantity can be found in [16] and [18].

3.3 Energy-based crack propagation criterion

Xie [7] derived an energy-based cohesive crack criterion for mixed-mode fracture, which is based on the principle of energy conservation

$$G - \mathbf{u}^T \frac{\partial \mathbf{f}}{\partial A} = 0 \quad (7)$$

where \mathbf{u} is the displacement vector, \mathbf{f} are the cohesive forces and A is the crack surface area. The total strain energy release rate G can be calculated as

$$G = -\frac{1}{2} \mathbf{u}^T \frac{\partial \mathbf{K}}{\partial A} \mathbf{u} + \mathbf{u}^T \frac{\partial \mathbf{P}}{\partial A} \quad (8)$$

with the stiffness matrix \mathbf{K} and the external nodal force vector \mathbf{P} . The computation of G is done by using the Virtual Crack Extension (VCE) according to [7]. The direction of the virtual crack is assumed to match with the direction of the last existing crack increment (Fig. 5). The crack tip node is shifted along this line for an infinitesimal virtual distance.

By assuming constant external forces the Mode-I and Mode-II components of $G = G_I + G_{II}$ can be obtained by using a finite difference approximation from Equation 8

$$G_I \approx -\frac{1}{2\Delta A} \left(\mathbf{u}_I^T \Delta \mathbf{K} \mathbf{u}_I \right)_{\Omega_{cr}}, \quad G_{II} \approx -\frac{1}{2\Delta A} \left(\mathbf{u}_{II}^T \Delta \mathbf{K} \mathbf{u}_{II} \right)_{\Omega_{cr}} \quad (9)$$

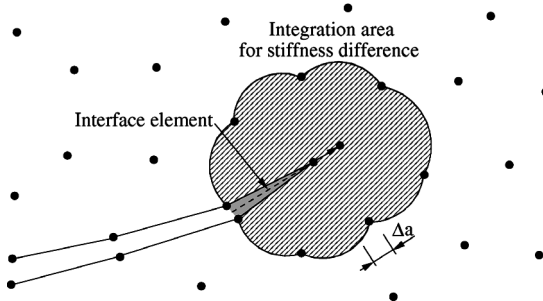


Figure 5. Virtual crack extension Δa at an existing crack tip with the NEM stiffness integration area (striped) and the observed cohesive interface element (gray).

\mathbf{u}_I and \mathbf{u}_{II} are the Mode-I and Mode-II displacements of the nodes in the crack tip area, Ω_{CT} , which are connected with the tip node in the meshless stiffness matrix. The stiffness difference can be easily computed from the integration points influenced by the crack tip node. The computation of \mathbf{u}_I and \mathbf{u}_{II} by using mirror images of the nodes is described in [19] in detail. The determination of the second term in Equation 7 is done by using finite difference approximations again

$$\mathbf{u}^T \frac{\partial \mathbf{f}}{\partial A} \approx \mathbf{u}^T \frac{\Delta \mathbf{f}_{CT}}{\Delta A} \quad (10)$$

where by only the cohesive interface element at the crack tip has to be considered [7]. The increase of the crack surface area ΔA is given for a 2D structure as the product of the virtual crack extension Δa and the thickness. The VCE according to [7] is shown exemplarily in Figure 5 with the NEM integration area to compute the stiffness difference.

This criterion is directly applicable only for existing crack tips. For crack initiation the stress-based criterion explained in section 3.2 is used. It is recommended in [7] to choose the direction of the crack propagation for the VCE method perpendicular to the direction of the maximum principal stress at the crack tip. A different crack direction criteria will be analyzed in section 5.2 based on the investigations in [20].

4 PROBABILISTIC MODEL

4.1 Random field modeling

The application of random fields in numerical computations requires the discretization of a continuous field. The application of point discretization methods shows several advantages compared with other methods, such as the simple computation of the correlation matrix and the matching distribution functions in the discretized and continuous case. In this study the integration point method is applied, where a random field is discretized at the integration points of the meshless zone. The random fields are assumed to be characterized by a given distribution type and a correlation function between the discrete random variables [8]. In this study an isotropic correlation type with an exponential correlation function is chosen exemplarily.

To simulate discrete samples of larger random fields, a reduction of the number of random variables could be necessary. This can be done by a transformation from an arbitrarily correlated space to the uncorrelated Gaussian space [8]. For non-Gaussian distribution types the Nataf transformation [21] has to be applied first to transform the correlation matrix C_{zz} to the correlated Gaussian space matrix C_{xx} . The transformation to the uncorrelated Gaussian space will be done by solving the standard eigenvalue problem

$$\mathbf{C}_{xx} = \Psi \mathbf{C}_{yy} \Psi^T = \Psi \text{diag}(\sigma_i^2) \Psi^T \quad (11)$$

where C_{yy} is the diagonalized correlation matrix, Ψ are the eigenvectors and σ_i^2 are the eigenvalues. To represent the random field with sufficient quality only a small number of the largest eigenvalues together with the corresponding eigenvectors is necessary. This number depends mainly on the correlation length.

To model different types of mutually correlated structural parameters at each discretization point, a given parameter correlation matrix has to be defined and will be combined point-wisely with the computed values of the geometrical correlation matrix.

4.2 Latin hypercube sampling

To determine the statistical characteristics of a structural response, Stratified Sampling methods can reach a sufficient accuracy with only a few samples if the number of uncorrelated random

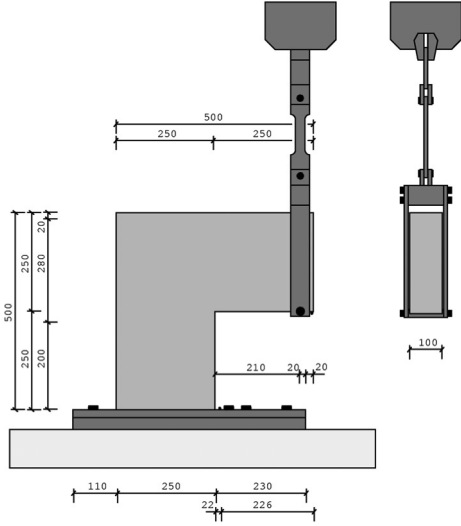


Figure 6. Test setup of the investigated L-shaped panel (Winkler 2001, dimension in *mm*).

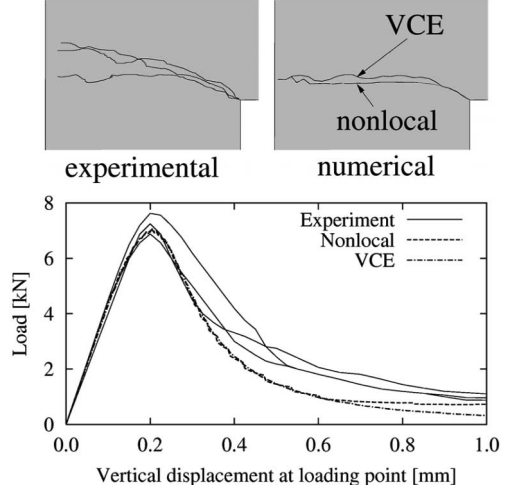


Figure 7. Experimental and numerical crack patterns and load displacement curves.

variables is small. One of these methods is Latin Hypercube Sampling (LHS) [9], which stratifies the theoretical probability distribution of the independent base variables x_i in N classes D_j

$$P[x_i \in D_j] = \frac{1}{N}; \quad j=1, \dots, N \quad (12)$$

For each class a representative value x_{ij} is chosen, the random variables are not simulated anymore. The obtained random permutation matrix has the size $N \times n$, whereby n is the number of pseudo-simulations. LHS was already successfully applied for nonlinear problems.

5 NUMERICAL EXAMPLES

5.1 Numerical investigation of L-shaped panel

Within this example the presented algorithm is used to predict curvilinear crack patterns. The verification of the algorithm for Mode-I problems with a theoretical straight crack line was shown by the authors in [20]. For this problem type the VCE criterion for crack growth and the principle of maximum hoop stresses [22] for the crack direction based on Linear Elastic Fracture Mechanics (LEFM) led to the best results. In this example the different criteria for crack growth and the crack direction will be investigated by analyzing a L-shaped concrete panel. In [23] three displacement controlled experimental tests have been carried out. The test setup is shown in Figure 6 and the experimental load displacement curves in Figure 7. The material parameters have been determined as follows: the Young's modulus as $2.6 \cdot 10^{10} N/m^2$ the Poisson's ratio as 0.18, the tensile strength as $2.7 \cdot 10^6 N/m^2$ and specific fracture energy in a range between 65 and 90 N/m . For the numerical investigations the Young's modulus was calibrated with the linear part of the load displacement curve with $1.8 \cdot 10^{10} N/m^2$ by using an initial uniform finite element discretization with 1200 4-node elements and 1281 nodes. The specific fracture energy was chosen analogous to the contribution of Oliver et. al. to [17] as 95 N/m which was determined from the test curves. The meshless calculation was done by using the initial finite element discretization and transforming those elements during the calculation to a meshless area, where the maximum principal stress of at least one integration point exceeds 90% of the tensile strength, and these, which are touched by a new crack

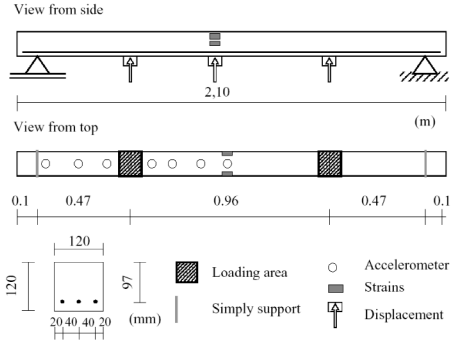


Figure 8. Simply supported reinforced concrete beam investigated numerically.

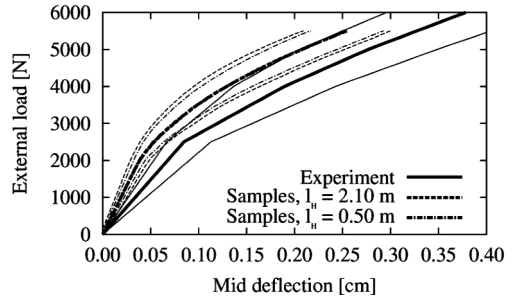


Figure 9. Statistical load displacement curves (thick line – means, thin line – standard errors).

increment. Details about this transformation have been published by the authors in [14]. In Figure 7 the obtained numerical results are displayed compared to the experimental values. The figure indicates a good agreement. For the calculation using the nonlocal crack propagation criterion the interaction radius was assumed as $R = 20 \text{ mm}$. The nonlocal load displacement curve shows an artificial stiffening effect above 0.7 mm vertical displacement caused by a strong oscillation at the end of the crack path.

5.2 Stochastic crack evaluation in a simply supported reinforced concrete beam

In this example the applicability of the presented stochastic model within the meshless formulation will be shown. For this purpose an experimentally investigated reinforced concrete beam [24] is analyzed numerically. Figure 8 shows the test setup with load and boundary conditions. The material parameters have been chosen analogous to [24]. The Young's modulus and the tensile strength of concrete are assumed to be the two parameters of a lognormally distributed random field. The coefficient of correlation between these parameters and the standard deviation were chosen as 0.8 and 0.2, respectively. To investigate the influence of the correlation length two different calculations with $l_H = 2.10 \text{ m}$ and $l_H = 0.50 \text{ m}$ were carried out by using 30 and 70 Latin Hypercube samples.

Figure 8 shows the load depending mean values and the standard deviations of the beam deflection for the experimental and the numerical investigations. The experimental results have been obtained by analyzing 20 test beams. The curves show good agreement in their trends. The different correlation lengths influence the standard deviations significantly, the influence on the mean values remains relatively small.

6 CONCLUSIONS

In this paper a discrete crack propagation algorithm is presented which uses the meshless Natural Neighbor Interpolation technique. The cohesive crack behavior of concrete is modeled by placing finite interface elements between the crack surfaces. Two different crack criteria are presented, a stress-based and a energy-based criterion. The latter one uses the Virtual Crack Extension technique to calculate the strain energy release rate as crack criterion and the principle of maximum hoop stress for the crack direction and gives more stable results than the stress criterion. The crack model was verified through the comparison with experimental data. The nonlinear behavior of concrete under compression which is not included in the model will be considered in further studies of the authors. A stochastic model using random fields is applied to represent the fluctuating material parameters. The required statistical analysis of the structural response is done using Latin

Hypercube Sampling to reduce the number of the necessary samples. The applicability of the stochastic model was shown on a further numerical example.

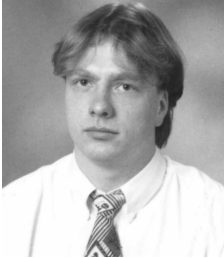
ACKNOWLEDGEMENT

This research has been supported by the German Research Council (DFG) through Collaborative Research Center 524, which is gratefully acknowledged by the authors.

REFERENCES

- [1] Moës, N., Dolbow, J. and Belytschko, T. 1999. A Finite Element Method for crack growth without remeshing. *International Journal of Numerical Methods in Engineering* 46: 131–150.
- [2] Belytschko, T., Kronkautz, Y., Organ, D., Fleming, M. and Krysl, P. 1996. Meshless methods: an overview and recent developments. *Comp. Methods in Applied Mechanics and Engineering*. 139: 3–48.
- [3] Sibson, R. 1980. A vector identity for the dirichlet tessellation. In *Mathematical Proceedings of the Cambridge Philosophical Society* 87, pages 151–155.
- [4] Belytschko, T., Lu, Y.Y. and Gu, L. 1994. Element-free Galerkin methods. *International Journal of Numerical Methods in Engineering* 37: 229–256.
- [5] Hillerborg, M., Modeer, M. and Peterson, P.E. 1976. Analysis of crack formation and crack growth in concrete by means of fracture mechanics and FE. *Cement and Concrete Research* 6: 773–782.
- [6] Rolshoven, S. and Jirásek, M. 2003. Numerical aspects of nonlocal plasticity with strain softening. In N. Bićanić et al., editors, *Proceedings EURO-C 2003*, St. Johann, Austria, March 17–20, Swets & Zeitlinger.
- [7] Xie, M. 1995. Finite element modelling of discrete crack propagation. PhD thesis, University of New Mexico, USA.
- [8] Brenner, C.E. 1995. Ein Beitrag zur Zuverlässigkeitsanalyse von Strukturen unter Berücksichtigung von Systemuntersuchungen mit Hilfe der Methode der SFE. PhD thesis, Univ. of Innsbruck, Austria.
- [9] Florian, A. 1992. An efficient sampling scheme: Updated Latin Hypercube Sampling. *Probabilistic Engineering Mechanics*, 7: 123–130.
- [10] Rubinstein, R.Y. 1981. *Simulation and the Monte Carlo Method*. John Wiley & Sons, New York.
- [11] Sukumar, N. 1998. *Natural Element Method in Solid Mechanics*. PhD thesis, Northwestern University, Illinois.
- [12] Unger, J.F. 2003. Development of an efficient algorithm for the application of the “Natural Neighbor Interpolation” for crack growth simulations. Diploma thesis, Bauhaus-Univ. Weimar, Germany.
- [13] Shewchuk, J.R. 1996. Triangle: A two-dimensional quality mesh generator and delaunay triangulator. Technical report, School of Computer Science, Carnegie Mellon University.
- [14] Most, T. and Bucher, C. 2003. “Moving Least Squares”-elements for stochastic crack propagation simulations coupled with stochastic finite elements. In A. Der Kiureghian et al., editors, *Proc. 9th Int. Conf. Appl. of Stat. and Prob. Civil Eng.*, San Francisco, July 6–9, Balkema, Rotterdam, 2003.
- [15] Herrmann, L.R. 1976. Laplacian-isoparametric grid generation scheme. *Journal Eng. Mech. Division, ASCE*, 102: 749–756.
- [16] Häußler-Combe, U. 2001. *Elementfreie Galerkin-Verfahren: Grundlagen und Einsatzmöglichkeiten zur Berechnung von Stahlbetontragwerken*. Habilitationsthesis, University of Karlsruhe, Germany.
- [17] NW-Ialad Integrity Assessment of Large Dams, 2003. <http://nw-ialad.uibk.ac.at>.
- [18] Most, T. 2003. Anwendung netzfreier Diskretisierungsverfahren zur stochastischen Rissfortschrittsberechnung. In Gebbeken, Bletzinger, and Rothert, editors, *Aktuelle Beiträge aus Baustatik und Comp. Mechanics*, 8. Forschungskolloquium Baustatik-Baupraxis 17–20. September 2003, Universität der Bundeswehr München.
- [19] Yang, Z.J., Chen, J.F. and Holt, G.D. 2001. Efficient calculation of stress intensity factors using virtual crack extension technique. *Computers and Structures* 79: 2705–2715.
- [20] Most, T., Bucher, C. and Unger, J.F. 2004. Stochastic modeling of cohesive crack propagation using meshless discretization techniques. In P. Neittaanmäki et al., editors, *Proc. 4th European Congress on Comp. Mechanics in Appl. Sciences and Eng.*, Jyväskylä, Finland, July 24–28, 2004.
- [21] Nataf, A. 1962. Détermination des distributions de probabilités dont les marges sont données. *Comptes Rendus de l’Academie des Sciences*, 225: 42–43.

- [22] Erdogan, F. and Sih, G.C. 1963. On the crack extension in plate under in plane loading and transverse shear. *Journal of Basic Engineering*, 85(4): 519–527.
- [23] Winkler, B.J. 2001. Traglastuntersuchungen von unbewehrten und bew. Betonstrukturen auf der Grundlage eines objektiven Werkstoffgesetzes für Beton. PhD thesis, Univ. of Innsbruck, Austria.
- [24] Ebert, M. and Bucher, C. 2002. Damage effects on the dynamic properties of R/C beams – experimental and numerical investigations. In H. Grundmann et al., (Eds.), *Proc. EUROLYN 2002*, Munich, Germany, September 2–5, 2002, Balkema, Rotterdam



Thomas Most, PhD Candidate

Bauhaus-University Weimar
Faculty of Civil Engineering
Institute of Structural Mechanics
Marienstr. 15
D-99423 Weimar, Germany
Tel.: +49 3643 584503
Fax: +49 3643 584514
E-mail: thomas.most@bauing.uni-weimar.de

Prof. Dr. techn. Christian Bucher, Supervisor

Bauhaus-University Weimar, E-mail: christian.bucher@bauing.uni-weimar.de